VAR a New Metric of Cryo-electron Tomography Resolution

Hmida Rojbani[1,2] and Atef Hamouda[2]
[1] *University of Strasbourg, 67412, Illkirch Cedex, France*
[2] *Faculty of Science of Tunis, University Tunis El Manar, 2092 El Manar Tunis, Tunisia*

Keywords: Electron Tomography, Resolution, Metric, 3*D* Structures, Tilt Angles.

Abstract: Motivate by reaching a better understanding of the biological cells, scientists use the **T**ransmission **E**lectron **M**icroscope (TEM) to investigate their inner structures. The cryo-electron tomography (cryo-ET) offers the possibility to reconstruct 3*D* structure reconstruction of a cell slice, that by tilting it according different angles. The resolution limits is the biggest challenge in the cryo-ET. The two phases involved in increasing the resolution are the acquisition phase and the reconstruction phase. In this work, we focus in the last one, as the biologists treat the acquisition phase within the phase of acquisition itself. The resolution of reconstruction depends on many factors such as: *(1)* the noisy and missing information from the collected projections data, *(2)* the capacity of processing large data sets, *(3)* the parametrization of the contrast function of the microscope, *(4)* errors of the tilt angles used in projections. In this paper, we presented a new method to evaluate the resolution of a reconstruction algorithm. Then the proposed method is used to show the relation between errors of the tilt angles used in projection and the degradation of the resolution. The resolution evaluation tests are made with different reconstruction methods (analytic and algebraic) applied on synthetic and real data.

1 INTRODUCTION

The resolution is a key characteristic of the 3*D* reconstructed object, it affects the visual quality of the object and it can limit the performance of the segmentation method if it fails to attain the highest level possible. The highest reachable resolution in cryo-ET is around 5Å, which allows us to locate small objects as ribosomes, nucleosomes, ... As requirement to achieve such resolution one must lower the dose of electrons used on the specimen during the acquisition and that to minimize the weight of radiation damage (Egerton et al., 2004). This reduction decreases the signal to noise ratio and delivers low contrast image. Moreover, the thickness of the ice used in the fixation of the sample affects also the final resolution of the reconstructed volume (Stagg et al., 2006). Therefore, the techniques requested to obtain high-resolution 3*D* structures must be refined in order to handle the low contrast and at the same time very noisy data (Sorzano et al., 2004).

Mainly, the reconstruction methods that are used in cryo-ET, they are belongs to two different family: (i) the analytic family, where we find methods as filtered back-projection methods, or direct Fourier inversion methods implemented in Fourier space (Penczek, 2010); (ii) the algebraic family, where iterative real-space methods are implemented, such as ART (Gordon et al., 1970) or SIRT (Gilbert, 1972).

In fact, we will focus in this paper on the resolution, specifically how we can judge if this resolution is a high resolution or not? The rest of the paper will be structured as follows: in section 2, we discuss the resolution in the literature, and we present the different method of reconstruction found in the literature in section 3. In section 4, we give our approach for judging the resolution quality; followed by presenting the evaluation of the results in section 5. Finally, we summarize and give some perspectives.

2 RESOLUTION: DEFINITION AND METHODS

One of the conversional question in the image-processing field is how we can define the resolution of an image. The term ”resolution” in its popular knowledge refers to the pixel count or the dimensions of an image. Unfortunately, this opinion has no real relation with the true meaning of the term resolution. Resolution is simply the ability to tell if a set of pixels represents distinct object rather than one object (*cf.* red

Rojbani, H. and Hamouda, A.
VAR a New Metric of Cryo-electron Tomography Resolution.
DOI: 10.5220/0005725801540159
In *Proceedings of the 11th Joint Conference on Computer Vision, Imaging and Computer Graphics Theory and Applications (VISIGRAPP 2016) - Volume 3: VISAPP*, pages 156-161
ISBN: 978-989-758-175-5

rectangles in Fig. 1).

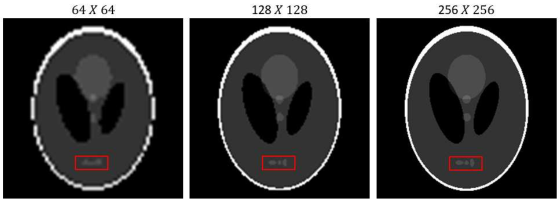

Figure 1: Effect of pixel resolution.

In electron microscopy, our field of interest, resolution (*A.K.A* spatial resolution) refers to the minimum distance between adjacent and in the same time distinguishable objects in the image; which can be both detected and interpreted (O'Keefe and Allard, 2004).

Another definition of spatial resolution is given by (Midgley and Weyland, 2003), where if the alignment condition of the projection images is satisfied, the resolution of the reconstructed object will be depends from number of projection used in the reconstruction (n_θ), maximum angle reached in the tilting operation (θ_{max}) (*cf.* Fig. 2) and the lateral dimension of the reconstructed volume (D). The resolution is different in each axis of the plan. Let us assume that that the object is in $OXYZ$ space, the axis of tilt is parallel to the axis OX and the electron beam is parallel to the OZ axis. Thus, it is possible to define the spatial resolution of the reconstructed volume along three plans as:

- XY: the resolution is equal to the resolution of the original $2D$ projections.
- XZ: the resolution is defined as $\pi D/n_\theta$.
- ZY: the resolution is degraded by a factor e_{yz} from the resolution of XZ. This factor is equal to :

$$e_{yz} = \sqrt{\frac{\theta_{max} + \sin\theta_{max}\cos\theta_{max}}{\theta_{max} - \sin\theta_{max}\cos\theta_{max}}}$$

We have another idea to determine the spatial resolution; our idea is based on a simulation of our visual experience with the image. The aim of proposing this new approach is to verify the truth of argument that said the uncertainty on the tilt angles due to mechanical imprecision of the TEM has no effect on the final reconstructed object resolution (Colliex, 1998). To test this theory, we used different reconstruction method that are presented in the next section.

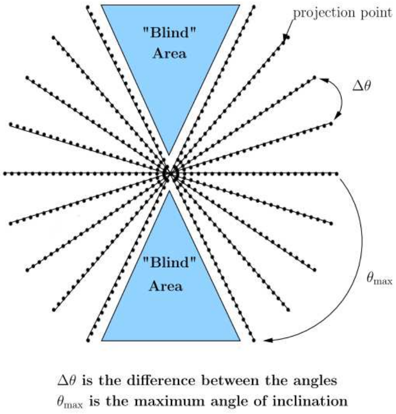

Figure 2: Illustration of sampling data in the Fourier space.

3 RECONSTRUCTION METHODS

In this section, we will discuss the commonly used methods in cryo-ET reconstruction. In general, there are two major families of tomographic reconstruction methods (Frank, 2006). One is the set of analytical algorithms, based on the direct data inversion. The other is the set of algebraic (iterative) methods, based on the inverse problem, which seeks to reconstruct the object by iteratively optimizing a criterion defining a range fidelity between the real projections data and the reconstructed object.

Analytical methods can use the fast Fourier transform in the calculation of the solution, which can accelerate the execution time of tomographic reconstruction. This is a considerable advantage compared to iterative methods. However, an analytical reconstruction will be effective only if the number of projection is high and they are uniformly distributed around the object, which is not the case of cryo-ET. Moreover, analytical methods are not adapted to the introduction of additional information on the object to be used in reconstruction to increase its effectiveness. For this reason, we will concentrate only on the algebraic reconstruction.

As mentioned above many algebraic reconstructions algorithm exist in the literature. In this paper, we will concentrate in how the model of pixels distribution in the projection are calculated, not in how the reconstruction algorithm works. In general, the problem of tomography represented by the relation between the projections $\mathbf{p}^{\theta_i}$ provided by the microscope according to angle θ_i and the reconstructed object $\mathbf{f}$, as follows:

$$\mathbf{p}^{\theta_i} = W_{\theta_i}\mathbf{f}, \tag{1}$$

Thereby, the projection problem is modeled as an equation system whose matrix W_{θ_i} is sparse. The matrix W_{θ_i} holds the coefficients of the projections according to the angle θ_i; $\forall i \in [1\ n_\theta]$. Here, our target is which is the best method to find W_{θ_i} or which method provide better resolution with a small number of projection (n_θ).

3.1 Modelisation of the Projection Matrix W_{θ_i}

A reconstruction of good quality requires accurate modelling of the data acquisition process, or the projection matrix. Several methods are proposed in the literature to model this matrix. Standard models such as ”voxel driven” and ”ray driven” (Joseph, 1982) are based on direct sampling, which gives modelling errors and artifacts in the reconstructed image. The model ”voxel driven” (*cf.* Fig. 3(a)) is based on connecting the source to the projection plane by passing a line through the middle of voxel of interest. However, the model ”ray driven” (*cf.* Fig. 3(b)) is based on connecting the source to the centre of the cell of interest on the projection plan by a passing a line through the image.

To overcome the shortcoming of these two algorithm, (Man and Basu, 2004) proposed another model called ”distance driven” that modelled the line projection in the shape of stairs to give a better modelling. This method’s role is to match the borders of each voxel and the borders of each cell of the projection plan on a common line; the difference between these points defines the projection coefficients. Measure the exact intersection area is a difficult task, for this reason, this area will be approximated. For example, to estimate the projection coefficient p_2 in Fig. 3(c), we can use the follow equation (Chen et al., 2015):

$$\Delta_{p_2} = \frac{(x_{n+1} - y_{m+1})\, f_1 + (y_{m+2} - x_{n+1})\, f_2}{y_{m+2} - y_{m+1}}$$

This is the usual method used in the cryo-ET algebraic reconstruction.

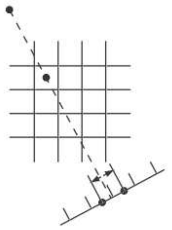

(a) ”voxel driven” (Man and Basu, 2004)

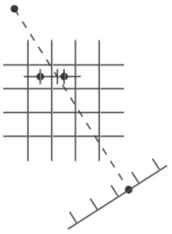

(b) ”ray driven” (Man and Basu, 2004)

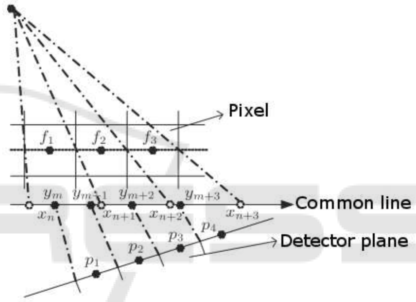

(c) ”distance driven” (Chen et al., 2015)

Figure 3: The various methods to create a projection matrix.

Recently, Momey *et al.* (Momey et al., 2011) proposed the use of B-splines as an alternative to the approach of ”distance driven” (*cf.* Fig. 3(c)). The B-Splines are piecewise polynomials, which are characterized by the degree of the constituent polynomials. The recent work of the sampling theory, (Thevenaz et al., 2000) (Unser, 2000), have demonstrated their effectiveness to represent a continuous signal with good accuracy. One of the most significant enhancements provided by the new approach ”spline driven” proposed by Momey *et al.* (Momey et al., 2014) is the reduction of the angular sampling projections without any quality loss. Indeed, this method is based on the idea of presenting the objects in the image by B-splines instead of using classical cubic grid. Even the lines of projections are modelled by B-splines. This model improves the calculation of the projection coefficients.

In this paper, we want to verify if the using of the iterative algebraic methods can affect and decrease the resolution of the reconstruction or not. For this, we will compare between SIRT (with the ”distance driven”) and the filtered back-projection (FBP), using our new metric of resolution. More details of this approach called **V**isual **A**ssumption of **R**esolution (VAR) is in the next section.

4 VISUAL ASSUMPTION OF RESOLUTION

The aim of using electron microscopy is reaching an atomic resolution, which is a hard target to reach in the biological imaging case, due to the sensibility nature of biological simples to electron radiation. The solution was to minimize in one side the electron dose used in acquisition (providing a low contrast image with low *SNR*) and in the other side the number of exposing to this dose (providing a small number of projection leading to a mediocre reconstruction). In this work, we will concentrate only on the effect of the projections number putting in mind that in the synthetic tests we will control everything else to be in the perfect conditions. The purpose of our metric VAR is to see how much is the loss of resolution according to the real objects resolution.

If we analyze visually the reconstructed object we find that the building shape of objects in the image change dramatically according to number of iteration of the reconstruction algorithm, the number of projection (n_θ) used in reconstruction (*cf.* Fig. 4). The changes can be described by perturbation in the borders of object, which leads to fusion of object if they are near each other. In addition, there are a slight change in the spectral of the object. Hence, we have the idea of using these two modification to calculate the rate of loss in resolution from the real object.

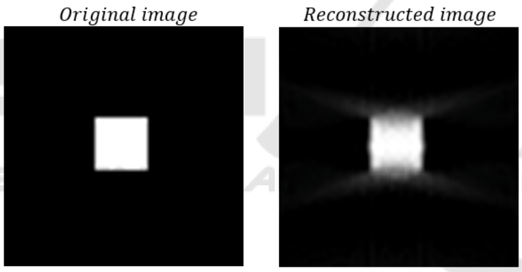

Figure 4: Resolution decrease after reconstruction with SIRT (100 iteration) and $n_\theta = 71$.

The VAR metric has two section, the first interpret the space (pixel) diversity between the original and reconstructed image (noted as VAR$_{space}$) and the second outline their the spectral (radiometry) variation (noted as VAR$_{spectral}$).

To calculate VAR$_{space}$ we will count the difference between the nonzero number of pixel in the original image and in the reconstructed image. The found value will be normalized by the nonzero number of pixel in the original image. The equation to calculate VAR$_{space}$ as follow:

$$VAR_{space} = \frac{|\sum_{i=1}^{\mathbf{N}} R_i - \sum_{i=1}^{\mathbf{N}} O_i|}{\sum_{i=1}^{\mathbf{N}} O_i} \quad (2)$$

Where **N** is the total number of pixel in the image, $R_i = 1$ (respectively $O_i = 1$) if the $i-$th pixel of the reconstructed (respectively original) image is nonzero, $R_i = 0$ (respectively $O_i = 0$) otherwise. VAR$_{space}$ will equal to zero if two image has the same number of nonzero pixels, otherwise will be greater than zero.

Now, to calculate VAR$_{spectral}$ we will count the difference between the sum of the spectral of all pixels between the original image and the reconstructed image. As the previous calculation, the difference will be normalized by the sum of the original image. The equation to calculate VAR$_{space}$ as follow:

$$VAR_{spectral} = \frac{|\sum_{i=1}^{\mathbf{N}} PxR_i - \sum_{i=1}^{\mathbf{N}} PxO_i|}{\sum_{i=1}^{\mathbf{N}} PxO_i} \quad (3)$$

Where PxR_i (respectively PxO_i) is the spectral of the $i-$th pixel of the reconstructed (respectively original). The same as the previous, VAR$_{spectral}$ will equal to zero if two image has the same amount of radiometries, otherwise will be greater than zero.

The value of VAR will be the mean between VAR$_{space}$ and VAR$_{spectral}$.

$$VAR = \frac{VAR_{space} + VAR_{spectral}}{2} \quad (4)$$

One can notice that for VAR to be efficient the tested image must simple structured. The tests and results of applying VAR in different situations are shown in the next section.

5 RESULTS

Several experiments were conducted to assess the efficiency of the proposed method on $2D$ and $3D$ data. The experiments involve 62 $2D$ and 25 $3D$ synthetic gray-level images randomly generated at different size $N = 128,\ 256,\ 512$. A sample of $2D$ the synthetic images used are shown in the figure 5.

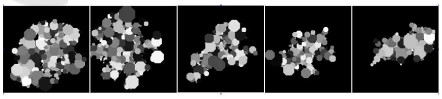

Figure 5: $2D$ synthetic images.

We will calculate also the cross-correlation coefficient (equation (5)). It is a criterion to measure the degree of similarity between the original image and the reconstructed image. This coefficient is equal to 1 when the reconstructed image coincides exactly with the original image and zero otherwise.

$$Corr = \frac{\sum_{i=1}^{\mathbf{N}} (PxO_i - M(O))(PxR_i - M(R))}{\sqrt{\sum_{i=1}^{\mathbf{N}} (PxO_i - M(O))^2 \sum_{k=1}^{\mathbf{N}} (PxR_i - M(R))^2}} \quad (5)$$

where $M(.)$ is the mean of the radiometry of the image.

The first phase of testing was to study the effect of different number projection (n_θ) over the resolution of the reconstruction. For the record, all the algebraic reconstruction in this section used a fixed number of iteration equals to 100 iterations. The mean results are shown in table 1 and table 2.

Table 1: The mean evaluation of 2D and 3D synthetic data for the FBP.

Size	128	256	512
Corr	0.89	0.93	0.95
VAR	0.67	0.59	0.58

Table 2: The mean evaluation of 2D and 3D synthetic data for the SIRT with ”distance driven” method.

Size	128	256	512
Corr	0.92	0.95	0.96
VAR	0.52	0.39	0.31

We can see clearly the upper hand of the SIRT over the FBP. Moreover, we notice in table 1 that even if the correlation is good, the resolution was poor. For this reason, we can say that correlation is not a trusted evaluation measure to prove the performance of a reconstruction. In the followed tests, we calculate only VAR.

The mean results according to deferent angular error (*AE*) applied on tilt angles are given in table 3 for $n_\theta = 360$ and in table 4 for $n_\theta = 71$, which is the usual number used in the real case of cryo-ET.

Table 3: The results for 3D synthetic data with $n_\theta = 360$.

AE	0°	$\leq 1^\circ$	$\leq 2^\circ$
FBP	0.56	0.88	0.92
SIRT	0.15	0.23	0.34

Table 4: The results for 3D synthetic data with $n_\theta = 71$.

AE	0°	$\leq 1^\circ$	$\leq 2^\circ$
FBP	0.82	0.99	1.32
SIRT	0.24	0.38	0.57

It is clear that if the tilt angles are erroneous, than the resolution will decrease even if we use all the possible tilt angles.

6 CONCLUSION

In this paper, we proposed a new metric to calculate the resolution of the reconstruction object. The purpose of this metric VAR is to verify to performance of the reconstruction algorithm used and their efficiency to preserve the resolution of the real object. We showed here, the upper hand of the algebraic iterative methods. In addition, we showed also the effect of an erroneous tilt angles over the results of the reconstructed object.

REFERENCES

Chen, J.-L., Li, L., Wang, L.-Y., Cai, A.-L., Xi, X.-Q., Zhang, H.-M., Li, J.-X., and Yan, B. (2015). Fast parallel algorithm for three-dimensional distance-driven model in iterative computed tomography reconstruction. *Chinese Physics B*, 24(2).

Colliex, C. (1998). *The Electron Microscopy*. Presses Universitaires de France.

Egerton, R., Li, P., and Malac, M. (2004). Radiation damage in the TEM and SEM. *Micron*, 35(6):399–409.

Frank, J. (2006). *Electron tomography: methods for three-dimensional visualization of structures in the cell*. Springer.

Gilbert, P. (1972). Iterative methods for the three-dimensional reconstruction of an object from projections. *Journal of Theoretical Biology*, 36(1):105–117.

Gordon, R., Bender, R., and Herman, G. (1970). Algebraic Reconstruction Techniques (ART) for three-dimensional electron microscopy and X-ray photography. *J Theor Biol*, 29(3):471–481.

Joseph, P. (1982). An improved algorithm for reprojecting rays through pixel images. *Medical Imaging, IEEE Transactions on*, 1(3):192–196.

Man, B. D. and Basu, S. (2004). Distance-driven projection and backprojection in three dimensions. *Physics in Medicine and Biology*, 49(11):2463.

Midgley, P. and Weyland, M. (2003). 3d electron microscopy in the physical sciences: the development of z-contrast and {EFTEM} tomography. *Ultramicroscopy*, 96(34):413 – 431. Proceedings of the International Workshop on Strategies and Advances in Atomic Level Spectroscopy and Analysis.

Momey, F., Denis, L., Mennessier, C., Thiebaut, E., Becker, J.-M., and Desbat, L. (2011). A new representation and projection model for tomography, based on separable b-splines. In *Nuclear Science Symposium and Medical Imaging Conference (NSS/MIC), 2011 IEEE*, pages 2602–2609.

Momey, F., Thiebaut, E., Mennessier, C., Denis, L., and Becker, J.-M. (2014). Spline driven: high accuracy projectors for 3D tomographic reconstruction from few projections. *submitted*.

O’Keefe, M. and Allard, L. (2004). A standard for sub-ngstrom metrology of resolution in aberration-corrected transmission electron microscopes. *Microscopy and Microanalysis*, 10:1002–1003.

Penczek, P. (2010). Chapter one - fundamentals of three-dimensional reconstruction from projections. In Grant, J., editor, *Cryo-EM, Part B: 3-D Reconstruction*, volume 482 of *Methods in Enzymology*, pages 1–33. Academic Press.

Sorzano, C., de la Fraga, L., Clackdoyle, R., and Carazo, J. (2004). Normalizing projection images: a study of image normalizing procedures for single particle three-dimensional electron microscopy. *Ultramicroscopy*, 101(24):129–138.

Stagg, S., Lander, G., Pulokas, J., Fellmann, D., Cheng, A., Quispe, J., Mallick, S., Avila, R., Carragher, B., and C.S.Potter (2006). Automated cryo-em data acquisition and analysis of 284742 particles of groel. *J Struct Biol*, 155:470–481.

Thevenaz, P., Blu, T., and Unser, M. (2000). Interpolation revisited [medical images application]. *Medical Imaging, IEEE Transactions on*, 19(7):739–758.

Unser, M. (2000). Sampling-50 years after shannon. *Proceedings of the IEEE*, 88(4):569–587.